

## MEDIUM MODIFICATION OF FRAGMENTATION FUNCTIONS

Pasquale Di Nezza  
INFN, Laboratori Nazionali di Frascati, I – 00044 Frascati, Italy  
dinezza@inf.infn.it

### Abstract

The influence of the nuclear medium on lepto-production of hadrons was studied in semi-inclusive deep-inelastic scattering off several nuclear targets. In particular, at the HERMES experiment at DESY, the differential multiplicity for krypton relative to that of deuterium has been measured for the first time for various identified hadrons ( $\pi^+$ ,  $\pi^-$ ,  $\pi^0$ ,  $K^+$ ,  $K^-$ ,  $p$  and anti- $p$ ) as a function of the virtual photon energy  $\nu$ , the fraction  $z$  of this energy transferred to the hadron, and the hadron transverse momentum squared  $p_t^2$ . The distribution of the hadron transverse momentum is broadened towards high  $p_t^2$  in the nuclear medium, in a manner resembling the Cronin effect previously observed in collisions of heavy ions and protons with nuclei. Moreover, by studying the hadron attenuation of the leading and sub-leading hadrons, it will be shown, for the first time, an additional tool for studying modifications of hadronization in nuclear matter.

### MODIFICACIÓN DEL MEDIO DE LAS FUNCIONES DE FRAGMENTACIÓN

### Resumen

La influencia del medio nuclear en la leptoproducción de hadrones se estudió en la dispersión semi-inclusiva profundamente inelástica de varios blancos nucleares. En particular, en el experimento HERMES en DESY, la multiplicidad diferencial del kriptón en relación con la del deuterio se midió por primera vez para varios hadrones identificados ( $\pi^+$ ,  $\pi^-$ ,  $\pi^0$ ,  $K^+$ ,  $K^-$ ,  $p$  y anti- $p$ ) como una función de la energía fotónica virtual  $\nu$ , la fracción  $z$  de esta energía transferida al hadrón y el cuadrado del momento transversal del hadrón  $p_t^2$ . La distribución del momento transversal del hadrón se ensancha hacia los  $p_t^2$  altos en el medio nuclear, de manera que semeja el efecto Cronin anteriormente observado en las colisiones de protones e iones pesados con los núcleos. Además, al estudiar la atenuación de los hadrones principales y sub-principales se mostrará por primera vez una herramienta adicional para el estudio de las modificaciones de la hadronización en materia nuclear.

*Key words: deep inelastic scattering, functions, heavy ion reactions, nuclear fragmentation, elementary particles, inelastic scattering, interactions, nuclear reactions, particle interactions, postulated particles, scattering, lepton-baryon interactions, lepton-hadron interactions*

### INTRODUCTION

The fragmentation process can be described by fragmentation functions  $D_i^h(z)$ , denoting the probability that a quark of flavor  $f$  produces a hadron of type  $h$  carrying a fraction  $z$  of the energy of the struck quark in the target rest frame [1]. In the nuclear medium additional soft processes may occur before the final-state hadron is completely formed influencing the hadronization process, e.g. causing a change in the quark fragmentation functions. The understanding of quark propagation in the nuclear medium is crucial for the interpretation of ultra-relativistic heavy ion collisions, as well as high energy proton-nucleus and lepton-nucleus interactions [2]. Quark propagation in the nuclear environment involves processes like energy loss of the propagating quarks, rescattering during the pre-hadronic formation process or interactions of the final-state hadrons within the nucleus. If the final hadron is formed inside the nucleus, the hadron can interact via the relevant hadronic interaction cross section, causing a further reduction of the hadron yield. Therefore, quark and hadron propagation in nuclei are expected to result in a modification i.e. a

“softening” of the leading-hadron spectra compared to that from a free nucleon. By studying the properties of the leading-hadrons emerging from nuclei, information on the characteristic time-distance scales of hadronization can be also derived.

In-medium modification of the quark fragmentation function has been described in terms of rescattering of gluons and quarks, and of energy loss due to induced gluon radiation [6,7]. Alternatively, colorless pre-hadron rescattering in the medium has been suggested [4,8] with additional effects due to  $Q^2$  rescaling [5]. Older interpretations [3] based on hadronic final-state interactions require a hadron formation length smaller than the nuclear size, which is unlikely for struck quarks boosted to energies larger than a few GeV. Although models based on some of these ideas are already in conflict with data, clearly other types of data are needed to further distinguish among these interpretations. In particular, the process of double-hadron production may be considered a tool to disentangle the inside-outside hadronization. If the absorption is the main contributor to nuclear suppression, naively one would expect the nuclear ratio for double-hadron production smaller compared to single-hadron production when this ratio is calculated on a nuclear target with respect

to the nucleon one. On the contrary, if the energy loss is the only mechanism involved, the double-hadron over single-hadron ratio in nucleus and deuterium is expected to be equal to the unity. Semi-inclusive deep-inelastic lepton-nucleus collisions are most suitable to obtain quantitative information on the hadronization process. In contrast to hadron-nucleus and nucleus-nucleus scattering, in deep-inelastic scattering no deconvolution of the parton distributions of the projectile and target particles is needed, so that hadron distributions and multiplicities from various nuclei can be directly related to nuclear effects in quark propagation and hadronization.

### Data Analysis

The experimental results for semi-inclusive deep-inelastic scattering on nuclei are presented in terms of the hadron multiplicity ratio  $R_M^h$ , which represents the ratio of the number of hadrons of type  $h$  produced per deep-inelastic scattering event on a nuclear target of mass  $A$  to that from a deuterium target ( $D$ ). The ratio  $R_M^h$  depends on the leptonic variables  $\nu$  and  $Q^2$ , which are the energy in the target rest frame and the squared four-momentum of the virtual photon respectively, and on the hadronic variables  $z = E_h/\nu$  and  $p_t^2$ , where  $p_t$  is the hadron momentum component transverse to the virtual photon direction. The multiplicity ratio is defined as:

$$R_M^h(z, \nu, p_t^2, Q^2) = \frac{\left. \frac{N_h(z, \nu, p_t^2, Q^2)}{N_e(\nu, Q^2)} \right|_A}{\left. \frac{N_h(z, \nu, p_t^2, Q^2)}{N_e(\nu, Q^2)} \right|_D}$$

where  $N_h$  is the yield of semi-inclusive hadrons in a given  $(z, \nu, p_t^2, Q^2)$ -bin, and  $N_e$  the yield of inclusive deep-inelastic scattering leptons in the same  $(\nu, Q^2)$ -bin.

The results on the hadron multiplicities on krypton relative to deuterium provides the first measurements of the multiplicity ratio for identified pions, kaons, protons and antiprotons [9].

The measurements described were performed with the HERMES spectrometer [10] using the 27.6 GeV positron beam stored in the HERA ring at DESY. The hadron identification was accomplished using the information from the RICH detector, which replaced a threshold Cerenkov counter used in the previously reported measurements on  $^{14}\text{N}$  [11].

The electromagnetic calorimeter provided neutral pion identification by the detection of neutral clusters originating from the two decay photons. Scattered positrons were selected by imposing the constraints  $Q^2 > 1 \text{ GeV}^2$ ,  $W > 2 \text{ GeV}$  for the invariant mass of the photon-nucleon system, and  $y = \nu/E < 0.85$  for the energy fraction of the virtual

photon. Contributions from target fragmentation were suppressed by requiring  $z > 0.2$ .

The data have been corrected for radiative processes involving nuclear elastic, quasi-elastic and inelastic scattering, using the code of references [12,13]. The code of reference [13] was modified to include the measured semi-inclusive deep-inelastic scattering cross section. The size of the radiative corrections applied to  $R_M^h$  was found to be negligible in most of the kinematical range, with a maximum of about 7% at the highest value of  $\nu$ , as most of the radiative contributions cancel in the multiplicity ratio.

The systematic uncertainty is reduced due to the fact that multiplicity ratios of semi-inclusive and inclusive yields are measured. To study the possibility to disentangle between the energy loss and absorption mechanism, the following double ratio for leading and sub-leading hadrons has been considered:

$$R_{zh}(z_2) = \frac{\left. \frac{dN^{z_1 > 0.5}(z_2)/dz_2}{N^{z_1 > 0.5}} \right|_A}{\left. \frac{dN^{z_1 > 0.5}(z_2)/dz_2}{N^{z_1 > 0.5}} \right|_D}$$

The values  $z_1$  and  $z_2$  correspond to the leading (largest  $z$ ) and sub-leading (second largest  $z$ ) hadrons, respectively. The quantity  $dN^{z_1 > 0.5}$  is the number of events with at least two detected hadrons in a bin of width  $dz_2$  at  $z_2$  with  $z_1 > 0.5$ . The quantity  $N^{z_1 > 0.5}$  is the number of events with at least one detected hadron with  $z_1 > 0.5$ . The label A(D) indicates that the term is calculated for a nuclear (deuterium) target.

Two methods of double-hadron event selection were used. Selection I contains only the combinations of hadron charges (leading-subleading) ++, --, +0, 0+, -0, 0-, 00. This suppresses the contributions from  $\rho^0 \rightarrow \pi^+\pi^-$  decay because the +- and +- combinations are missing. Moreover, in the Lund string model, the exclusion of the opposite-charge combinations enhances the rank-1 (leading) plus rank-3 (sub-leading) combination. The higher the particle rank, the more likely it is formed deep inside the nucleus, and the corresponding hadron absorption should be larger. Selection II contains all particle charge combinations. Here, the sub-leading hadron is mainly of rank-2 and the contribution from  $\rho^0$  decay is larger.

### RESULTS AND INTERPRETATIONS

The multiplicity ratio has been determined as a function of either  $z$ ,  $\nu$  or  $p_t^2$ , while integrating over all other kinematical variables. In figure 1-left the multiplicity ratios for all charged hadrons with  $z > 0.2$  are presented as a function of  $\nu$  together

with data of previous experiments on nuclei of similar size. In the top panel the HERMES data on Kr are compared with the SLAC [14] and CERN [15] data for Cu. In the lower panel the reevaluated HERMES data on  $^{14}\text{N}$  are displayed together with data on  $^{12}\text{C}$  [15]. The HERMES data for  $R_M^h$  are observed to increase with increasing  $\nu$ , roughly approaching the EMC results at higher values of  $\nu$ . The discrepancy with the SLAC data is partially due to the fact that semi-inclusive cross section ratios were measured at SLAC instead of multiplicity ratios. Thus no corrections in the SLAC data were made for the target-mass dependence of the inclusive deep-inelastic scattering cross section, as discussed in [17].

A stronger attenuation is observed for Kr than for  $^{14}\text{N}$ , the average ratios and the total experimental uncertainties being  $R_M^h=0.802 \pm 0.021$  and  $R_M^h=0.954 \pm 0.023$ , respectively.

Figure 1-right shows the dependence on  $z$  of the same multiplicity ratios for  $\nu > 7$  GeV. This figure includes the region  $z < 0.2$ , which contains contributions from both target fragmentation hadrons and leading hadrons decelerated in nuclear re-scattering.

The measured  $\nu$ - and  $z$ -dependences for both krypton and nitrogen are compared to several model

calculations. In reference [5] the nuclear modification of hadron production in deep-inelastic scattering is described as a rescaling of the quark fragmentation functions, supplemented by nuclear absorption. In reference [7] nuclear modification of the quark fragmentation process in deep-inelastic scattering has been evaluated taking into account multiple parton scattering and induced energy loss in the medium.

For the first time the  $z$ - and  $\nu$ -dependences of the multiplicity ratio were also studied for identified neutral and charged pions, kaons, protons and antiprotons, as shown in figure 2. The results for all identified hadrons are compared to the calculations of reference [4].

The results presented in figure 2 show that the multiplicity ratios for positive and negative pions are similar and consistent with the multiplicity ratio for neutral pions. However,  $R_M^h$  for positive kaons is significantly larger. An even larger difference is observed between protons and their antiparticles compared to the meson case. It has been suggested [7] that the observed differences in  $R_M^h$  can be attributed to the mixing of quark and gluon fragmentation functions.

This mixing gives a different modification of the quark and antiquark fragmentation functions in nuclei, thus leading to a more significant

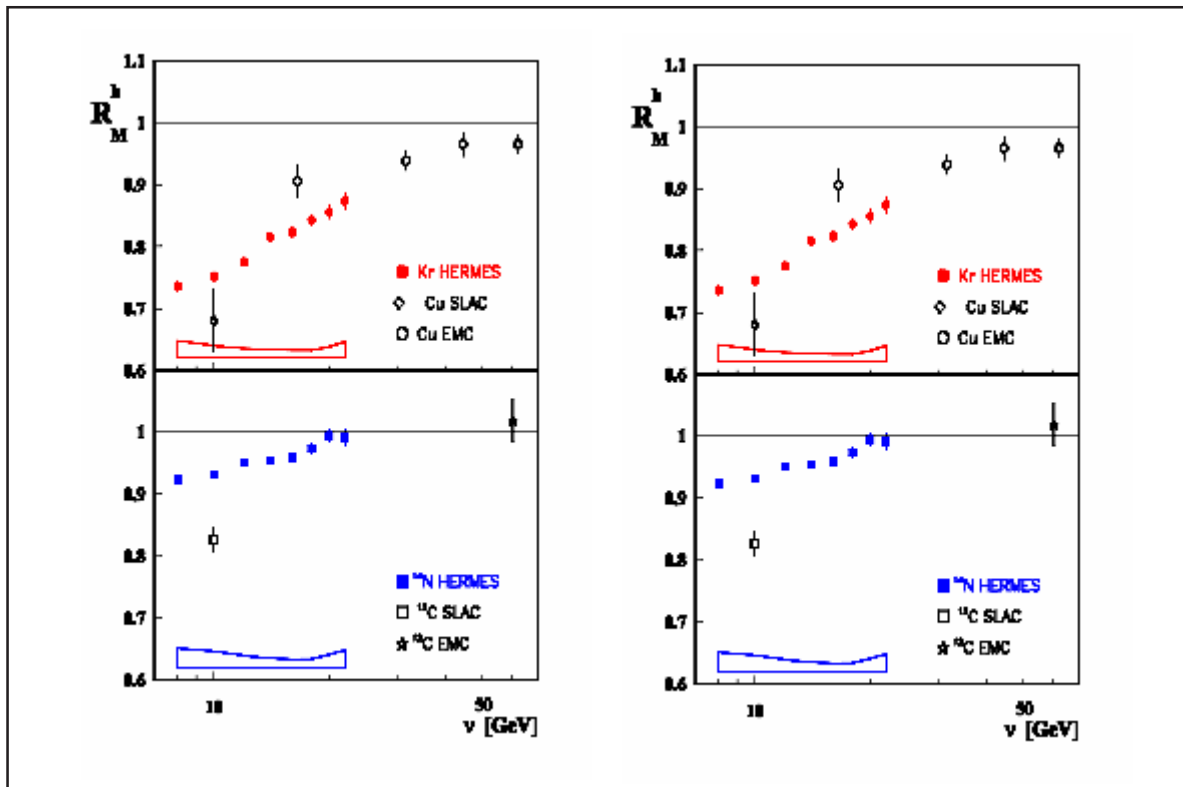


Figure 1. (Left) Charged hadron multiplicity ratio  $R_M^h$  as a function of  $\nu$  for  $z > 0.2$ . In the upper panel HERMES data on Kr are compared to SLAC [14] and CERN [15] data on Cu. In the lower panel the HERMES data on  $^{14}\text{N}$  are compared with CERN and SLAC data on  $^{12}\text{C}$ . (Right) Charged hadron multiplicities  $R_M^h$  as a function of  $z$  for  $\nu > 7$  GeV. The error bars represent the statistical uncertainties, while the systematic uncertainty is shown as the band.

difference between the multiplicity ratio of protons and antiprotons than between those of mesons. The observed differences in the multiplicity ratios can also be interpreted in terms of different formation times of baryons and mesons [16], or in terms of different hadron-nucleon interaction cross sections. While this cross section is similar for positive and negative pions, it is larger for negative kaons as compared to positive kaons, and even larger for antiprotons than protons, in qualitative agreement with the trend shown by the data.

The  $p_t$  distribution of the observed hadrons is expected to be broadened on a nuclear target compared to a proton target due to multiple scattering of the propagating quark and hadron.

This effect is known as the Cronin effect [17] and has previously been observed in heavy-ion and hadron-nucleus induced reactions. A nuclear enhancement at high  $p_t^2$  is also observed in the HERMES data as shown in figure 3 both for  $^{14}\text{N}$  and Kr nuclei. In this plot the EMC [15] data on Cu which cover a different  $\nu$ -range,  $10 < \nu < 80$  GeV, are also displayed. The data for  $p_t^2 < 0.7$  GeV $^2$  show the attenuation previously discussed, while the data for  $p_t^2 > 0.7$  GeV $^2$  reflect the  $p_t$ -broadening ascribed to multiple scattering effects. This effect is similar to the one reported for proton-nucleus and nucleus-nucleus collisions [18] but is smaller in

magnitude. The enhancement is also predicted to occur at a  $p_t$ -scale of about 1-2 GeV [19-20], in agreement with the semi-inclusive deep-inelastic scattering data shown in figure 3. The HERMES data may help to interpret the new relativistic heavy-ion results from SPS [21] and RHIC [22], which show a weaker  $p_t$  enhancement than expected from the original Cronin effect, due to the fact that, in the first, only Final State Interactions can contribute.

Figure 4 shows the double ratio  $R_{2h}$  as a function of  $z_2$  for Selection I only [23].  $R_{2h}$  is generally below unity with no significant difference between the three nuclei. These data clearly show that the nuclear effect in the double-hadron ratio is much smaller than for the single-hadron attenuation measured under the same kinematic conditions [1,9]. For  $z_2 < 0.1$ , where  $R_{2h}$  rises towards and possibly above 1, the slow hadrons originate largely from target fragmentation [4]. Also for  $z_2 > 0.4$ , where the two hadrons have similar energy,  $R_{2h}$  seems to rise towards unity. Figure 4 (upper panel) shows calculations based on a PYTHIA event generator with a fully coupled-channel treatment of final-state interactions by means of a BUU transport model [4]. In this model, the fragmentation function is modified by pre-hadron interactions and rescattering in the medium. Although the general trend of the data is

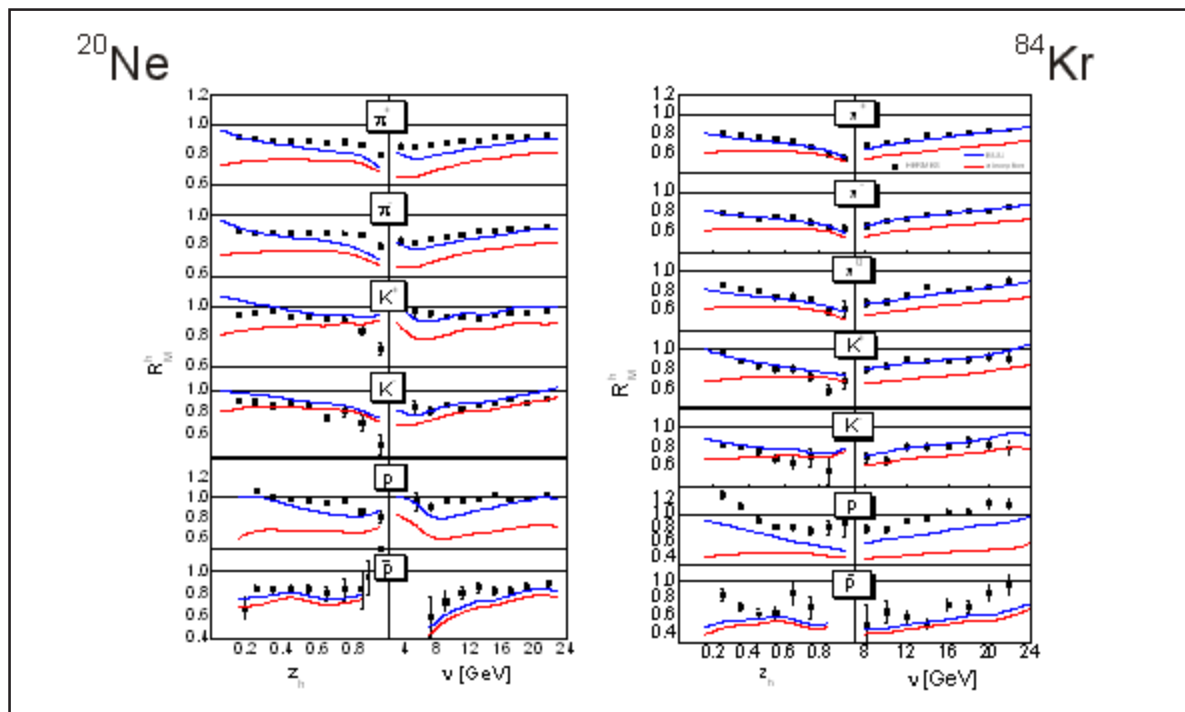


Figure 2. Multiplicity ratios, measure at HERMES [9], for identified pions, kaons, protons and antiprotons from a Ne (left) and Kr target (right) as a function of  $\nu$  and  $z$ . The blue curves represent a calculation [4] for the pre-hadronic cross section and a formation time  $t_f = 0.5$  fm/c, while the red curves represent the same calculation with a purely absorptive treatment of the Final State Interactions.

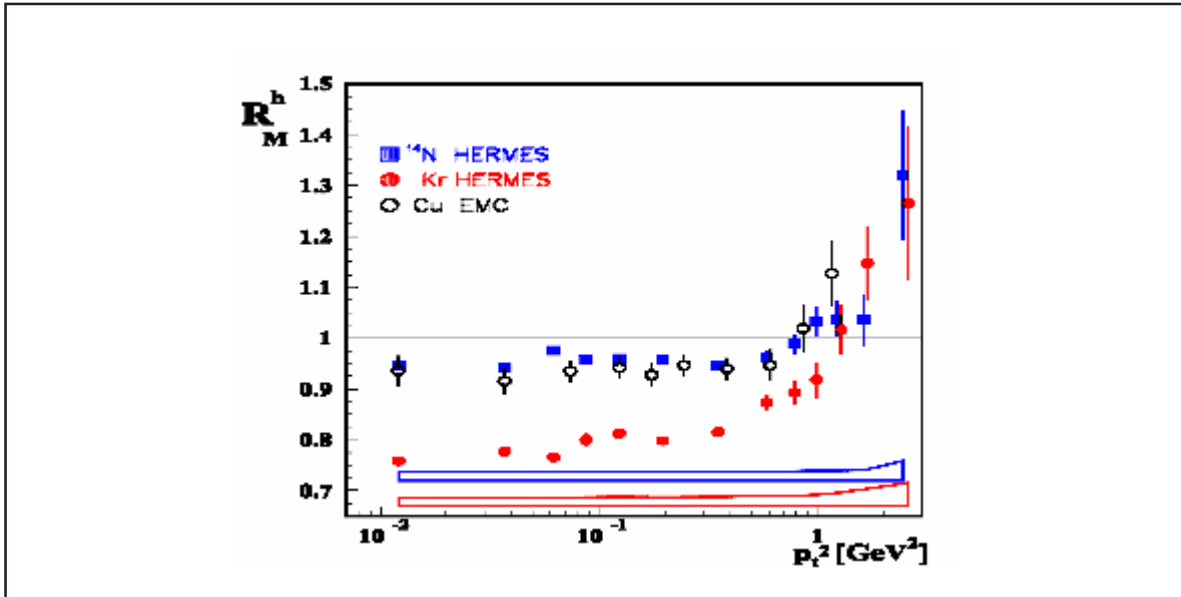


Figure 3. Multiplicity ratio for charged hadrons versus  $p_t^2$  for  $v > 7$  GeV and  $z > 0.2$ . The HERMES data on Kr and  $^{14}\text{N}$  are compared to the EMC [15] data for Cu taken in the range  $10 < v < 80$  GeV. The error bars represent the statistical uncertainties, while the systematic uncertainty for Kr ( $^{14}\text{N}$ ) is shown as the lower (upper) band.

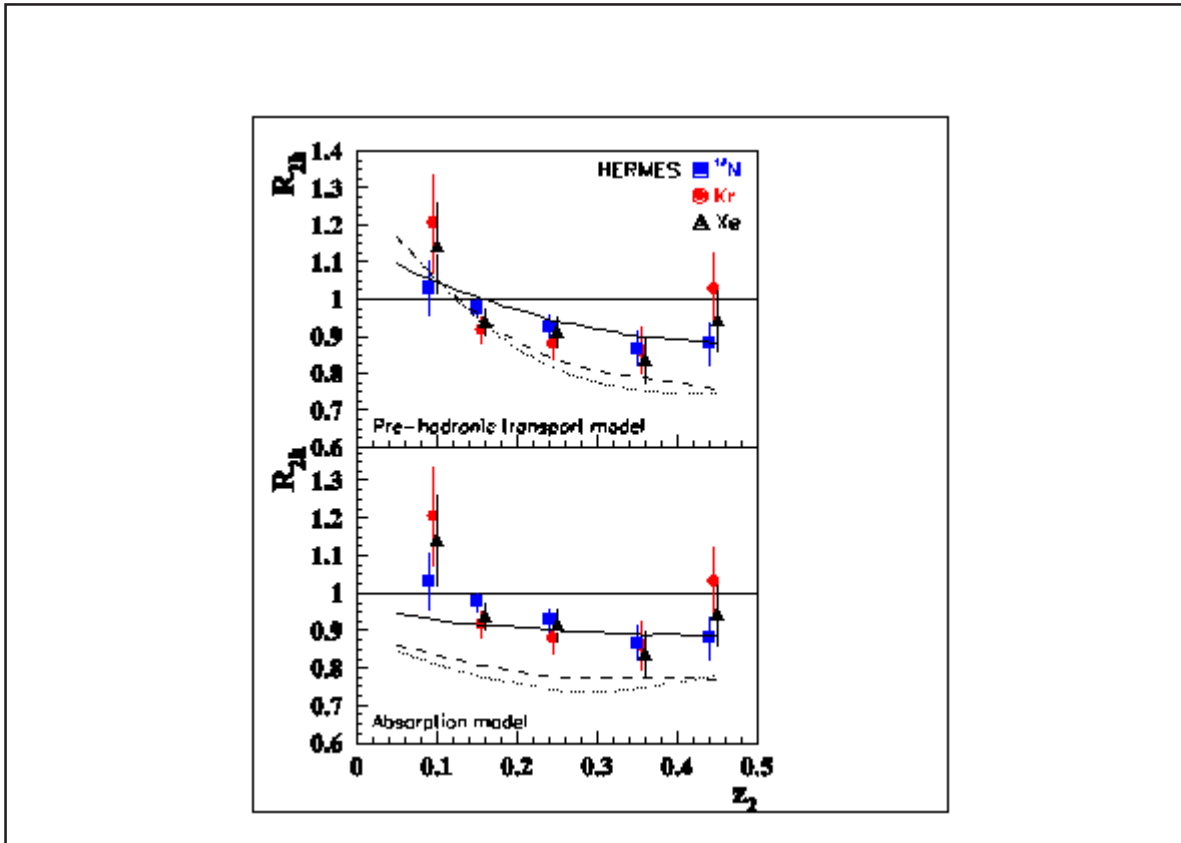


Figure 4. The ratio  $R_{2h}$  as a function of  $z_2$  for  $^{14}\text{N}$  (squares), Kr (circles) and Xe (triangles) with  $z_1 > 0.5$ . Only Selection I was considered. The systematical uncertainty is 2% for all the targets and is independent of  $z_2$ . In the upper panel the curves (solid for  $^{14}\text{N}$ , dashed for Kr, dotted for Xe) are calculated within a BUU transport model [4]. In the bottom panel the same data are shown with calculations that assume only absorption for the three nuclei (same line types as in the upper plot) [4].

reproduced, the model predicts an effect twice as large for xenon and krypton as for nitrogen above  $z_p = 0.1$ , which is not supported by the data. Figure 4 (bottom panel) shows the same data compared to a calculation with a purely absorptive treatment of the interaction of the pre-hadronic or the final hadronic states. The data rule out this assumption [4].

### CONCLUSION

The multiplicities of charged hadrons and of identified pions, kaons, protons and antiprotons on various nuclei relative to deuterium were measured for the first time. The data show that the multiplicity ratio  $R_M^h$  is reduced at low  $n$  and high  $z$ . Different multiplicity ratios were observed for various hadrons. In contrast to the similarity between positive and negative pions, a significant difference in  $R_M^h$  is found between positive and negative kaons and a larger difference between protons and antiprotons. The different results for various hadrons may reflect differences in the modification of quark and antiquark fragmentation functions and/or in the hadron nucleon interaction cross sections. The hadron multiplicity is observed to be enhanced at high  $p_t^2$  in the nuclear medium, showing evidence of the Cronin effect in deep-inelastic scattering process. This effect is similar to the one observed in hadron nucleus scattering, with a rise of  $R_M^h$  to values above unity for  $p_t^2 > 1 \text{ GeV}^2$ . The ratio of double- to single-hadron yields from nuclear targets compared to deuterium are similar for atomic mass numbers  $A = 14, 84$  and  $131$ , as a function of the relative energy of the sub-leading hadron. The data do not support naive expectations for pre-hadronic and hadronic final-state interactions that are purely absorptive. Models that interpret modifications to fragmentation as being due to pre-hadronic scattering or partonic energy loss are also inconsistent with the data. Like measurements in heavy-ion collisions, the double-hadron observables in semi-inclusive deep inelastic scattering provide new information for differentiating between models of hadronization in nuclei that are indistinguishable in single-hadron measurements.

### REFERENCES

- [1] HERMES Coll., A. Airapetian *et al.*, Eur.Phys.J. C21 (2001)599-606.
- [2] BAIER, R., SCHIFF, D., ZAKHAROV, B.G., Ann. Rev. of Nucl. and Part. Science 50 (2000)37.
- [3] BIALAS, A. Acta Phys. Pol. B11 (1980)475.
- [4] FALTER, T., *et al.*, Phys. Lett. B 594 (2004)61; Phys. Rev. C 70 (2004)054609; GALLMEISTER, K., and CASSING, W. Nucl. Phys. A 748 (2005)241; GALLMEISTER, K., FALTER, T. Phys. Lett. B 630 (2005)40; private communication.
- [5] ACCARDI, A., MUCCIFORA, V. PIRNER, H. J. Nucl. Phys. A 720 (2003)131.
- [6] ARLEO, F. JHEP 11 (2002)44; Nucl. Phys. A 715 (2003)899.
- [7] WANG, X.N., GUO, X., Nucl. Phys. A 696 (2001) 788; WANG, E., WANG, X.N. Phys. Rev. Lett. 89 (2002)162301 WANG X.N. private communication.
- [8] KOPELIOVICH, B.Z. NEMCHIK, J. PREDAZZI, E., HAYASHIGAKI, A., Nucl. Phys. A 740 (2004)211.
- [9] HERMES Coll, AIRAPETIAN, A., *et al.*, Phys. Lett. B 577 (2003)37.
- [10] HERMES Coll., ACKERSTAFF, K., *et al.*, Nucl. Instr. and Meth. A 417 (1998)230.
- [11] HERMES Coll., AIRAPETIAN, A. *et al.*, Eur. Phys. J. C 20 (2001)479.
- [12] AKHUNDOV, A.A., BARDIN, D. YU, SHUMEIKO, N.M. Sov. J. Nucl. Phys. 26 (1977)660; BARDIN, D.YU., SHUMEIKO, N.M. Sov. J. Nucl. Phys. 29 (1979)499; AKHUNDOV, A., *et al.* Sov. J. Nucl. Phys. 44 (1986)988.
- [13] AKUSHEVICH, I. SHUMEIKO, N., SOROKO, A. Eur. Phys. J. C 10 (1999)681.
- [14] OSBORNE, L.S. *et al.*, Phys. Rev. Lett. 40 (1978)1624.
- [15] EMC Coll., ASHMAN, J. *et al.*, Z. Phys. C 52 (1991) 1.
- [16] KOPELIOVICH, B.Z., NIEDERMAYER, F. Phys. Lett. B 151 (1985)437.
- [17] CRONIN, J.W., *et al.*, Phys. Rev. D 11 (1975)3105.
- [18] WA98 Coll., AGGARWAL, M.M. *et al.*, Phys. Rev. Lett. 81 (1998)4087 and 84 (2000)578(E); NA49 Coll., APPELSHAUSER, H. *et al.*, Phys. Rev. Lett. 82 (1999)2471; CERES Coll., AGAKISHIEV, G., *et al.*, hep-ex/0003012.
- [19] WANG, E., X.N. Wang, Phys. Rev. C 64 (2001)034901.
- [20] KOPELIOVICH, B.Z. *et al.*, Phys. Rev. Lett. 88, (2002)232303.
- [21] WA98 Coll., AGGARWAL, M.M. *et al.*, Eur. Phys. J. C 23 (2002)225.
- [22] PHENIX Coll., ADCOX, K., *et al.*, Phys. Rev. Lett. 88 (2002)022301.
- [23] HERMES Coll., AIRAPETIAN, A. *et al.*, Phys. Rev. Lett. 96 (2006)162301.

Recibido : 15 de enero de 2007

Aceptado : 1 de noviembre de 2007